Tetrahedron 66 (2010) 605–611

Contents lists available at ScienceDirect

Tetrahedron

journal homepage: www.elsevier.com/locate/tet

Imino–enamine tautomerism and dynamic prototropy in 1-imino-3-amino-1*H*-indens

Yoko Mukano, Mai Momochi, Yuriko Takanashi, Mitsuaki Suzuki, Hidetsugu Wakabayashi, Hiroyuki Teramae, Keiji Kobayashi *

Department of Chemistry, Graduate School of Material Science, Josai University, Keyakidai 1-1, Sakado, Saitama 350-0295, Japan

ARTICLE INFO

Article history:
Received 29 October 2009
Received in revised form
17 November 2009
Accepted 17 November 2009
Available online 20 November 2009

ABSTRACT

The tautomeric structures and dynamic prototropic behavior of the products **1** and **2** obtained in the condensation reaction of 1,3-indandione and 2-pyridyl-1,3-indandione with *p*-toluidine, respectively, were investigated by ^{1}H NMR spectroscopy and X-ray analysis. In the solid state, compound **1** is in an imino–enamine tautomeric form, whereas in solution it coexists with an imino–imino tautomeric form. Dynamic 1,5-prototropic interconversion of the imino–enamine form was revealed to be very fast at room temperature by temperature-dependent ^{1}H NMR spectra. For **2**, the imino–enamine form is the only species present in solution. The hydrogen of the enamine NH is hydrogen-bonded intramolecularly with the nitrogen in the pyridine ring. When the temperature is raised, the NH proton enters into dynamic 1,5-migration, which is accompanied by internal rotation around the pivot bond, which changes the hydrogen-bonding sites. For the condensation product **3** of 2-(2-quinolyl)-1,3-indandione with *p*-butylaniline, dynamic behavior similar to that found in **2** was observed also in ^{13}C NMR spectra.

1. Introduction

Prototropic imino–enamine tautomerism has been extensively investigated in porphyrins,[1] azaannulenes,[1,2] and indigodiimine[3] in which the NH hydrogen is hydrogen-bonded intramolecularly with the basic nitrogen and the degenerate imino–enamine tautomerism takes place as double or multiple proton transfer in combination with degenerated reorganization of the cyclic π-conjugation. Such proton migration may be formally expressed as 1,5-prototropy in general scheme A (Scheme 1). Dynamic nature in this type of prototropy has been recognized not only in solution but also in the solid state.[4] Annular tautomerism observed in 1,5-diaza-heterocycles may also be regarded as formal imino–enamine 1,5-prototropy. A relevant example is represented by pyrazole as B in Scheme 1.[5,6] In contrast to type A, hydrogen bonding plays no role in type B, besides multiple proton transfer between the neighboring molecules aligned in the solid state.[4,6]

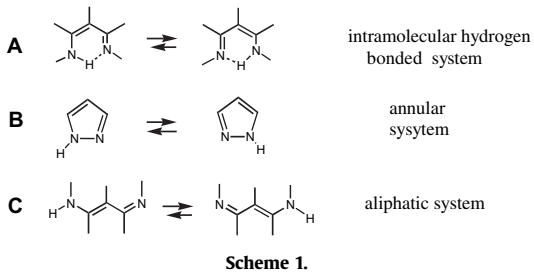

Scheme 1.

Despite the wealth of information available for the 1,5-prototropic imino–enamine tautomerism in heterocyclic systems,[7] much less is known about those in acyclic systems such as the prototropic tautomerism represented by general scheme C in Scheme 1. This tautomeric system is a vinylogue of 1,3-prototropy in amidine and related compounds,[8,9] on which several studies have been carried out. The difficulties encountered in investigating 1,5-prototropy in acyclic systems like C are configurational and conformational problems that should be disclosed prior to discussion of prototropic behavior. Therefore, to fix the configuration unambiguously, we designed an imino–enamine tautomeric system incorporating the 1,3-indandione framework. In this paper, we report tautomeric and prototropic properties in the compounds **1**–**3** of type C obtained by the condensation reaction of 1,3-indandione, 2-(2-pyridyl)-1,3-indandione, and 2-(2-quinolyl)-1,3-indandione with *p*-alkyl anilines, respectively, and a peculiar example of dynamic 1,5-proton transfer accompanied with bond rotation observed in **2** and **3**.

* Corresponding author.
E-mail address: kobayak@josai.ac.jp (K. Kobayashi).

0040-4020/$ – see front matter © 2009 Elsevier Ltd. All rights reserved.
doi:10.1016/j.tet.2009.11.076

2. Results and discussion

2.1. 1-Imino-3-amino-1*H*-inden system bearing no substituent on C2 carbon (1)

Compound **1** was prepared by the condensation reaction of 1,3-indandion with *p*-toluidine. Its structure was confirmed by X-ray analysis (Fig. 1). In the crystalline state **1** exists in an imino–enamine form on the basis of that a hydrogen atom is unequivocally located close to the one of the nitrogen atoms and the two C–N bond lengths are not equivalent (1.370 and 1.297 Å). Thus, compound **1** contains a planar –NH–C═C–C═N– substructure. The tolyl group linked to the imino nitrogen is directed to the opposite side with respect to the benzene ring of the indan unit, represented as *trans* configuration. The tolyl ring linked to the amino nitrogen takes the *s-trans* conformation as well, represented as *anti* conformation. In the crystalline state, molecules of **1** are linked by intermolecular NH···N hydrogen bonds (N···N: 2.996 Å), resulting in a linear chain arrangement.

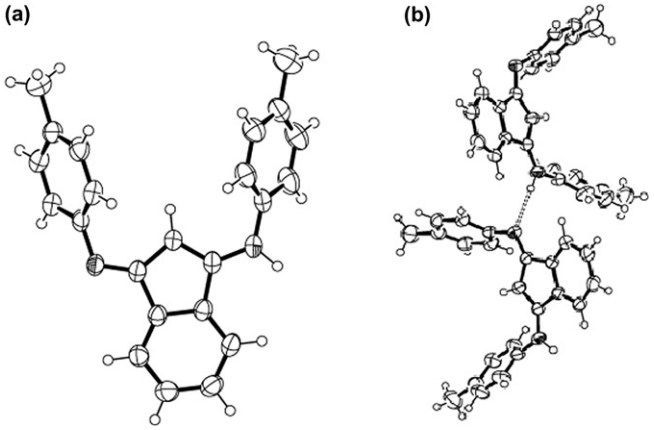

Figure 1. X-ray structure of **1**: (a) molecular structure and (b) molecular arrangement.

In contrast to the solid-state structure, in solution compound **1** coexisted with diimino form **4** as evidenced by its NMR spectrum (Scheme 2). The presence of **4** is established on the basis of the observation of methylene signal at 3.15 ppm and of the symmetric A_2B_2 signals of the aromatic region in the indan fragment. At the same time, **1** showed a signal attributed to an enamine-type proton at 5.65 ppm. In Figure 2, the ^{1}H NMR spectra are shown for **1** and **4** individually, and for clarity, the signals of the other species have been erased. On the basis of the signal intensities, the ratio of **1**:**4** was estimated to be 3:1. The ^{13}C NMR spectra also revealed the involvement of the two tautomeric forms, showing the methylene carbon signal of **4** at 33 ppm and the sp^2 carbon (C2) signal of **1** at 89 ppm.

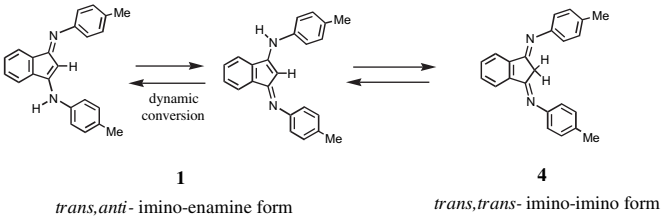

Scheme 2.

By analyzing the NMR spectrum of **1**, the structure of **1** can be deduced more precisely. If **1** is assigned a *trans*-imino and *anti*-amino structure, the aromatic hydrogens of the indan subunit should exhibit NMR signals in an ABXY pattern because of the magnetic nonequivalence of these protons. However, this was not the case: a symmetric A_2B_2 profile was observed at 7.55 and 7.41 ppm as rather broad signals (Fig. 2). Furthermore, the two tolyl rings substituted on the amino- and imino-nitrogens cannot be distinguished, because they have the same chemical shifts. These observations indicate that molecule **1** is represented at room temperature by a time-averaged structure of two imino–enamine forms because of fast 1,5-proton migration. The ^{13}C NMR spectrum is also consistent with this interpretation. There are 12 observable signals in the aromatic region including the benzene ring of the indan framework, although this is less than the 14 signals due to the presence of **1** (seven signals) and **4** (seven signals). Decreasing the temperature to −80 °C in CD_2Cl_2 resulted in substantial broadening of the ^{1}H NMR signals, but no decoalescence was observed, indicating the low barrier of this prototropy on the NMR time scale. Furthermore, no significant change in population of **1** and **4** was observed in the variable-temperature NMR, showing that **1** is slightly more stable than **4** by 0.12 kJ mol^{-1}.

The question of whether proton migration occurs by intermolecular double proton transfer in a dimeric- or multimolecular alignment caused by hydrogen bonding between mutual H-donating and H-acceptor sites arises. If the tolylimino moiety is in the *cis* configuration, such-self association, as illustrated in Scheme 3, would be possible. For **1**, however, the *trans* configuration of the C═N bond is

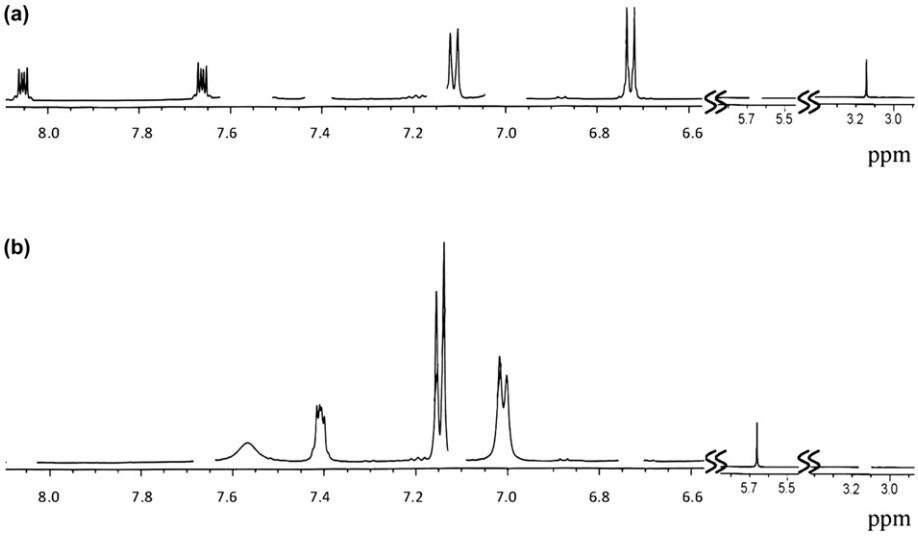

Figure 2. ^{1}H NMR spectra of **1**, showing two tautomers present in CD_2Cl_2. Signals of the other species have been erased: (a) diimino form **4** and (b) imino–enamine form **1**.

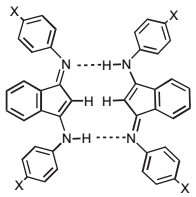

Scheme 3.

realized, which would prevent self-association because of significant steric hindrance. Moreover, changing concentration for NMR measurements caused no effect on the chemical shifts, indicating that self-association is not involved. When a few drops of D_2O were added to the acetonitrile-D_3 solution of a tautomeric mixture of **1** and **4**, the NH signal broadened remarkably in a few minutes, whereas neither the =CH proton of **1** nor the $-CH_2-$ protons of **4** entered into deuterium exchange. These observations indicate that the 1,5-prototropy does not involve sequential 1,3-migration, but occurs directly between the enamine and imino nitrogen atoms. In other words, the 1,5-prototropy is faster than the prototropic tautomerism between the imino–enamine and imino–imino forms.

The structural outcome of **1** and **4** in solution was supported by theoretical calculations at a B3LYP/6–31G(d, p) level, which were carried out for simplicity on the molecule with no methyl substituents (Fig. 3). For the imino–enamine form, the *trans*, *anti* isomer was calculated to be the most stable with the *trans, syn* form the next, being higher by 11.7 kJ mol^{-1}. The stability of the *trans*, *anti* configuration may be ascribed to a decrease in steric hindrance compared with the *cis* and *syn* arrangement. In agreement with this, for the diimino tautomer, the *trans*, *trans* configuration was shown to be the most stable structure. The calculated energies of the *trans*, *anti* imino–enamine form and the *trans*, *trans*-diimino form are almost equivalent, the difference being only 4.2 kJ mol^{-1}. These results justify the presence of diimino form **4** and imino–enamine form **1** in solution, though far from quantitatively.

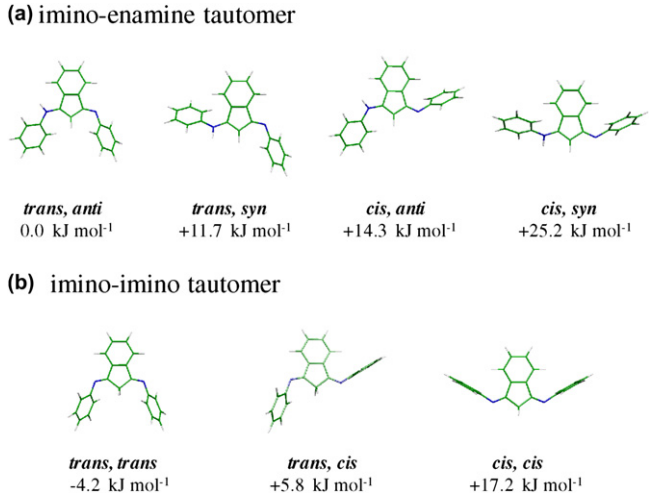

Figure 3. Optimized structures of the tautomers and their relative energies: (a) imino–enamine form **1** and (b) imino–imino form **4**.

2.2. Protonation to 1

As described above, the NMR data revealed the involvement of equilibrium between the imino–enamine tautomer **1** and the diimino tautomer **4** and dynamic interconversion in the imino–enamine tautomers due to 1,5-prototropy. One may suspect then that the NMR characteristics observed in imino–enamine tautomer **1** are not due to proton migration but may be interpreted in terms of protonation brought about by chance in the protic out-of-molecule environment. However, such an interpretation is not reasonable. The hydrochloride salt of **1** was isolated by crystallization in the presence of hydrochloric acid and its ^{1}H NMR spectrum was easily distinguishable from that of neutral **1** (Fig. 4 (c)). The most characteristic feature of the NMR spectrum of (**1**H$^+$)(Cl$^-$) is low-field shift of the *peri* hydrogens of the indan moiety down to 8.3 ppm.

The X-ray analysis was carried out for a single crystal of (**1**H$^+$)(Cl$^-$). The ionic structure of (**1**H$^+$) was similar to that reported for (**1**H$^+$)(ClO_4^-).[10] The aniline moieties are directed away from the benzene ring of the indan framework as observed in the neutral crystals (Fig. 5). The C_1=N$^+$ and C_3=N$^+$ bond lengths are comparable, being 1.327 and 1.321 Å, respectively, which are intermediate values between those of the C_1=N and C_3–N bonds in neutral **1**. The

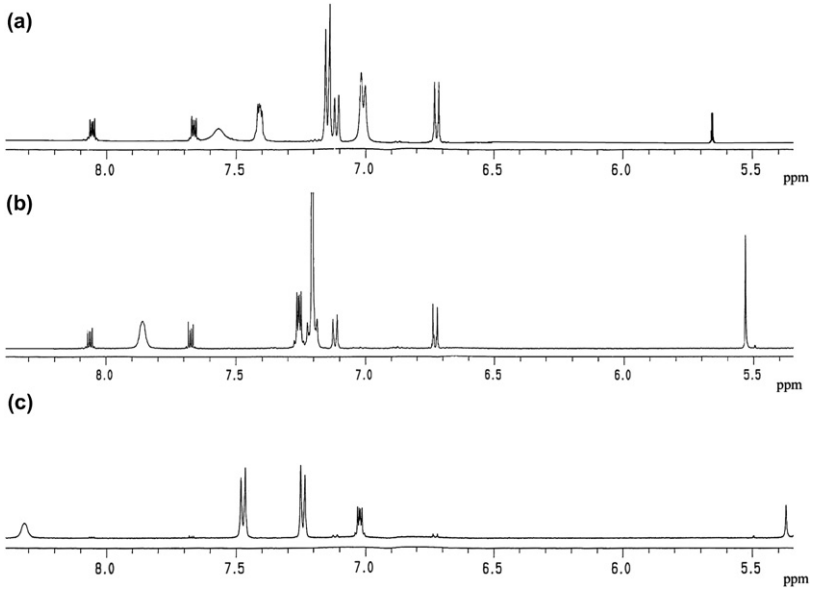

Figure 4. ^{1}H NMR spectra observed when the following samples are dissolved in CD_2Cl_2. (a) **1**, indicating presence of **4**. (b) 1:1 mixture of **1** and (**1**H$^+$)(Cl$^-$), showing disappearance of half of **4**. (c) solution of (**1**H$^+$)(Cl$^-$).

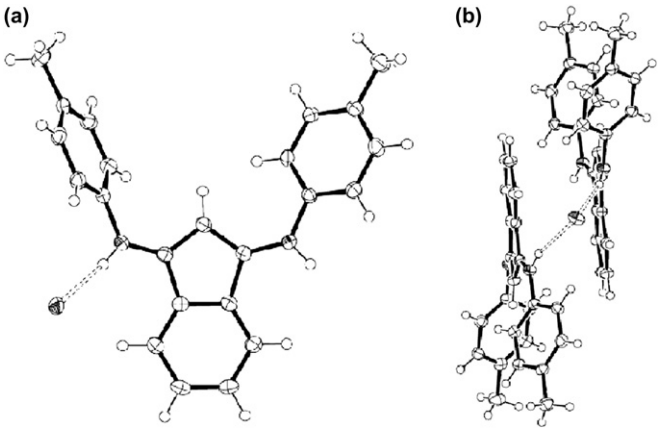

Figure 5. X-ray structure of (**1**H$^+$)(Cl$^-$). (a) Molecular structure and (b) molecular arrangement.

structural features also hold for the C_1–C_2 and C_2–C_3 bonds (1.395 and 1.397 Å, respectively). On the other hand, the crystal structure of (**1**H$^+$)(Cl$^-$) is different from that of (**1**H$^+$)(ClO_4^-). In (**1**H$^+$)(Cl$^-$), the chloride anion is hydrogen bonded with the =N$^+$H hydrogens to link two (**1**H$^+$) species (NH···Cl$^-$:2.30 Å), affording a dimeric unit of (**1**H$^+$)(Cl$^-$) (Fig. 5). Thus, one of two NH groups is not involved in hydrogen bonding.

With the hydrochloride of **1** in hand, we investigated the dependence of existing species on proton concentration by adding (**1**H$^+$)(Cl$^-$), instead of hydrochloric acid, to a dichloromethane solution in which **1** and **4** coexist in a 3:1 ratio. A 1:1 mixture of **1** and (**1**H$^+$)(Cl$^-$) should provide a solution of **1** containing the acid in half molar quantity of **1**. The ^{1}H NMR spectrum of this solution is shown in Figure 4 (b). The most interesting feature is the decrease of **4** to half of the original population, indicating that **4** is transformed to a protonated species by a fraction of the added protons. Moreover, the protonated species is not stationary (**1**H$^+$) but is in dynamic equilibrium with **1**. This is evident from the observation that the original signals of **1** without acid merge with those of (**1**H$^+$)(Cl$^-$) and gradually shift depending on the quantity of acid and ultimately coincide with those of 100% protonated (**1**H$^+$)(Cl$^-$). Similar behavior of **1** was observed by adding trifluoroacetic acid to a dichloromethane solution of **1**.

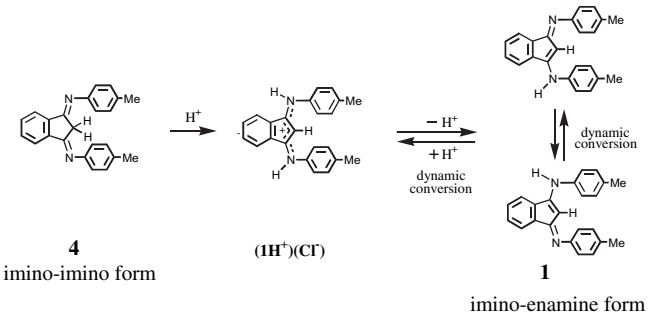

Scheme 4.

Two conclusions may be drawn from these observations. First, protonation of the nitrogen of **4** enhances the acidity of its methylene hydrogens to induce tautomerization and result in the stoichiometric conversion of **4** to (**1**H$^+$)(Cl$^-$). Second, intramolecular dynamic proton migration, which occurs in the neutral form of **1**, is further expanded to include intermolecular proton transfer with (**1**H$^+$)(Cl$^-$). This implies that not only intramolecular prototropy in **1** but also the protonation–deprotonation equilibrium is induced between (**1**H$^+$)(Cl$^-$) and **1** by adding acid, which results in the fast dynamic conversion of these species (Scheme 4).

2.3. 2-(2-Pyridyl) derivative (2)

In compound **1**, the two aniline rings are in the *trans*, *anti* form. It would be interesting to investigate tautomeric and prototropic behavior of the *cis*, *syn* form compared with that of the *trans*, *anti* form. In the condensation product of 2-(2-pyridyl)-1,3-indandione with *p*-toluidine, such a tautomeric structure has been realized. The X-ray analysis of **2** showed that (1) compound **2** exists as an imino–enamine tautomeric structure; (2) the imino and amino moieties adopt *cis* and *syn* orientations, respectively; (3) the amino hydrogen has intramolecular hydrogen bonding with the nitrogen of the pyridine ring; and (4) the molecules are in a flip-flop disorder, being co-crystallized with molecules arranged at 180° rotations around the longest molecular axis including the indan unit (Fig. 6). As a result of intramolecular hydrogen bonding, the pyridine ring is coplanar with the indan ring. Thus, the C_1=N (C_3=N) bond distance is 1.315 Å, which is shorter than a typical C–N bond but longer than a typical C=N bond. It is also true for the C_1–C_2 and C_2–C_3 bonds.

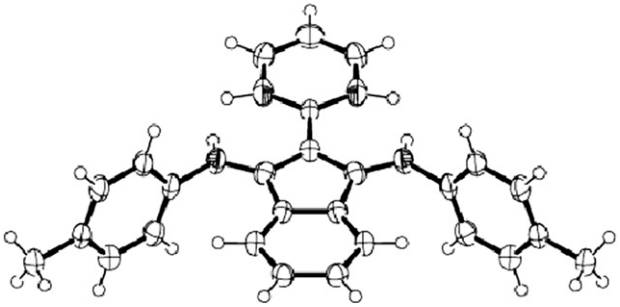

Figure 6. X-ray structure of **2**.

The structure of **2** determined by X-ray analysis was consistent with the results from the DFT calculation carried out by removing the methyl substituents (Fig. 7): the optimized structure is the *cis*, *syn* form, which is more stable than the other three forms by more than 16 kJ mol^{-1}. The indan subunit is coplanar with the pyridine ring, also in accordance with the X-ray results.

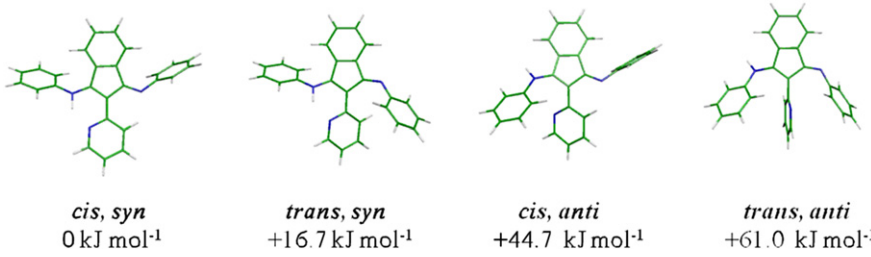

Figure 7. Optimized structures of **2**.

The ^{1}H NMR spectrum of **2** in $CDCl_2CDCl_2$ indicates that **2** is an imino–enamine in solution, which is apparent from the occurrence of a signal due to the hydrogen-bonded NH proton at 12.6 ppm and of four nonequivalent signals of an ABXY pattern due to the aromatic protons of the indan framework. No other signal attributable to a diimino form was observed. When the temperature was increased, the ABXY signals of the indan unit and the four doublets due to *p*-methylanilino moieties were broadened. In contrast to these signals, those of the pyridine moieties are not markedly affected by increasing temperature. Throughout the whole temperature range, the chemical shift of the NH proton showed no significant change, remaining at approximately 14 ppm, but its signal was broadened. At 90 °C the two doublet signals of the indan unit (AB part) coalesce (Fig. 8). These observations clearly indicate that compound **2** is in dynamic equilibrium between degenerated imino–enamine structures through the 1,5-migration of the NH proton accompanied by rotation about the pivot bond connecting the pyridine and indan frameworks. The NH proton is kept in the intramolecular hydrogen bond in the ground state, implying that the NH proton migrates rapidly between the two nitrogen atoms and changes its hydrogen-bonding site (Scheme 5). Note that the molecular structure of **2** in the crystalline state occurs in static disorder resulting in *Cs* symmetry for the averaged structure. In solution, such disorder appears dynamic. A free energy barrier ($\Delta;G^{\ddagger}$) for this dynamic process was roughly estimated by the coalescence method to be 73 kJ mol^{-1} at 90 °C.[11]

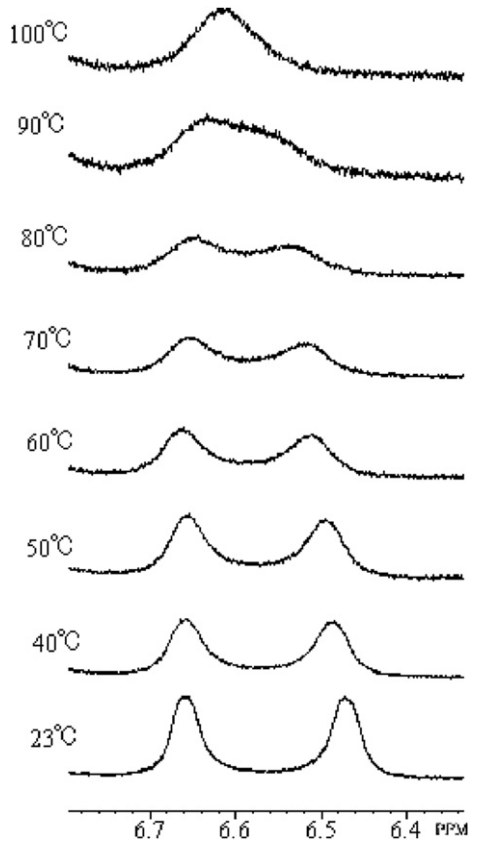

Figure 8. Variable temperature ^{1}H NMR of **2** in $CDCl_2CDCl_2$.

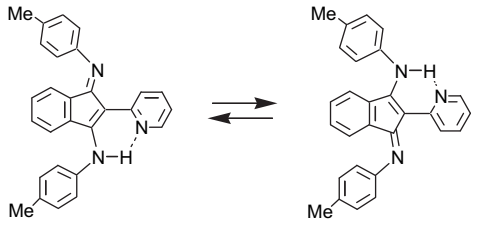

2

Scheme 5.

The dynamic behavior found in compound **2** is analogous to that of tautomeric system A of Scheme 1 in the sense that cleavage of intramolecular hydrogen bonds participates in prototropy. It would be rational to assume that the activation energy of the dynamic process estimated for **2** is required for the dissociation of the NH···N intramolecular hydrogen bond. The 1,5-prototropy in the *trans*, *anti*-1-imino-3-amino-1*H*-inden system, i.e., system C in Scheme 1, is fast as revealed in **1**. Therefore, once the hydrogen bond is broken, the exchange of the hydrogen-bonding site by 1,5-prototropy is accomplished prior to the reformation of the intermolecular hydrogen bond. In fact, addition of D_2O to the acetone-D_6 solution of **2** resulted in the disappearance of the NH proton, whereas other signals in the ^{1}H NMR spectrum were not affected at all. Dynamic prototropy, which has been reported recently for 1*H*-perimidine-2-carbxylate, would be analogous to the present case, since 1,3-prototropy is synchronized with bond rotation to exchange hydrogen-bonding sites with the carbonyl carbon.[12] Throughout this study we could not find any evidence for the existence of the tautomeric structure represented by canonical structure **5**. This is in contrast to the corresponding diketo compound, which has been reported to prefer keto-enamine tautomeric structure **6** in the crystalline state as well as in solution[13] (Scheme 6).

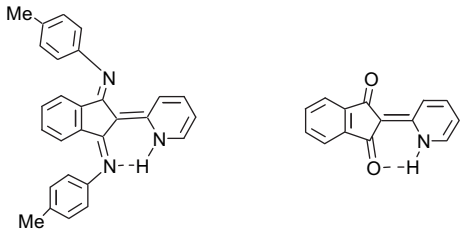

5 **6**

Scheme 6.

2.4. 2-(2-Quinolyl) derivative (3)

Dynamic behavior similar to that found in **2** was also recognized in quinoline substituted derivative **3**. The ^{1}H NMR spectrum of **3** indicates that the condensation product exists in solution as imino–enamine tautomeric structure **3** based on assignment of all the signals in an H–H COSY experiment and by recognizing the aromatic region of the indan unit as an ABXY spin system. Unfortunately, X-ray analysis could not be conducted for **3**, because single crystals suited for X-ray diffraction could not be obtained. However, the optimized structure based on DFT calculations supported that tautomers with *cis* configuration and *syn* conformation are the most stable structure, as shown in **2** (Scheme 7).

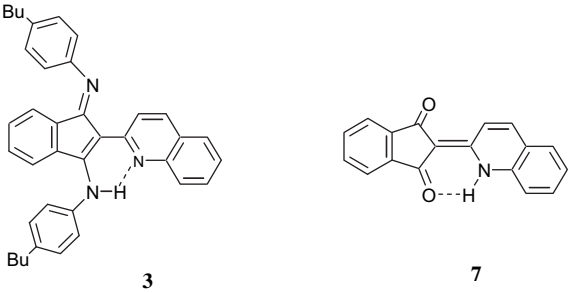

3 **7**

Scheme 7.

Dynamic behavior of **3** was investigated by variable temperature ^{13}C NMR. At room temperature, compound **3** displays 26 signals in $CDCl_3$ due to the imino–enamine tautomeric structure. The signals of the butyl carbons occurred in four sets between 10 and 40 ppm, each of which is comprised of two slightly separated peaks due to different magnetic environments in the *p*-butylphenyl-amino and -imino substituents. The signals at 35.09 and 35.17 ppm were assigned to the α carbon of the butyl group on the basis of HMQC experiments (Fig. 9). It is interesting to note that the β-carbon of the butyl group shows the most significant magnetic nonequivalence among its four ^{13}C resonances of the butyl group in contrast to the appearance in ^{1}H NMR.[14] Therefore, these peaks were monitored in variable temperature experiments using $CDCl_2CDCl_2$ as solvent. With increasing temperature, two signals at 33.50 and 33.81 ppm become broadened and coalesce at 63 °C. The free energy barrier at this coalescence temperature was calculated based on a coalescence method to be 66.2 kJ mol^{-1} at 63 °C. The dynamic behavior of **3** could be compared with that of the diketo derivative **7** corresponding to a precursor of **3**.[15]

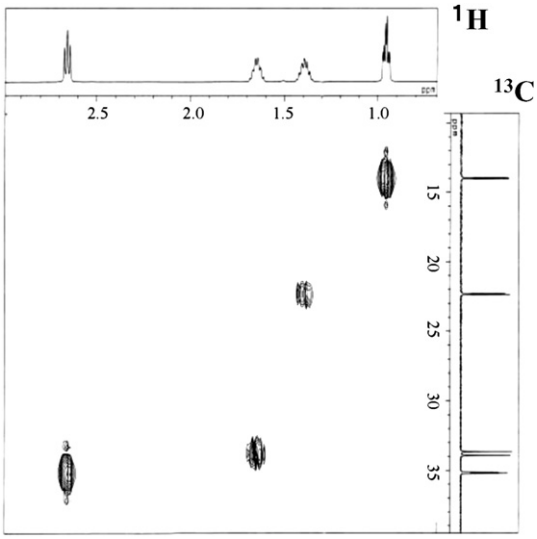

Figure 9. HMQC spectrum of **3** in the aliphatic carbon region.

3. Conclusions

We have described the tautomeric preference and 1,5-prototropy in acyclic and non-heterocyclic imino–enamine systems by designing molecules that possess the configurationally fixed framework. The product obtained by the condensation reaction of 1,3-indandione with *p*-toluidine, **1**, exists in imino–enamine tautomeric form in the solid state, whereas, in solution the imino–imino form is present. In the imino–enamine tautomer, dynamic 1,5-sigmatropy between the two degenerate imino–enamine structures occurs, which is fast on the NMR time scale even under −80 °C. When acid is added, the imino–imino form in solution is converted to the imino–enamine form by a stoichiometric amount of acid, and both species interconvert rapidly to show an averaged structure in the NMR spectrum. The solid-state structure of the condensation product of 2-(2-pyridyl)-1,3-indandion with *p*-toluidine is the imino–enamine form, in which the hydrogen of the enamine NH is hydrogen-bonded intramolecularly to the nitrogen in the pyridine ring. This tautomeric form is the only species present in solution. The NH proton participates in dynamic 1,5-migration when the temperature is raised, which is accompanied by internal rotation around the pivot bond. A similar dynamic behavior was observed for the quinolyl derivative and the activation energy of prototropy was estimated.

4. Experimental

4.1. General

All the melting points were determined using a Yanaco MS-500 V apparatus and are uncorrected. The ^{1}H NMR (500 MHz) and ^{13}C NMR (125 MHz) spectra were recorded using a JEOL α-500 spectrometer. Chemical shifts are given in δ values (ppm) using TMS as the internal standard. Mass spectra were taken on a Shimadzu GC–MS-QP5050A mass spectrometer. Elementary combustion analyses were recorded using a Yanaco CHN CORDER MT-6 analyzer. All reactions were monitored by TLC employing a 0.25 mm silica gel plate (Merck 60F_{254}). Column chromatography was carried out on silica gel (Merck 60N spherical). The yields of products are based on the initial weights of the 1,3-indandiones.

*4.1.1. 1-(p-Tolylimino)-3-(p-tolylamino)-1H-inden (**1**).* To a solution of 1,3-indandione (3.03 g, 20.7 mmol) in acetic acid (80 mL) was added *p*-toluidine (4.88 g, 45.7 mmol) at room temperature. The mixture was heated at reflux for 4 h. After cooling, saturated NaCl aqueous solution (ca. 500 mL) was added and the resulting solid was collected by filtration and dried in vacuo. The solid was divided into three portions, and each was chromatographed through a silica gel column using benzene–methanol (10:1) as the eluent to afford crude **1** as a yellow solid. The crude product, combined from three portions, was purified by recrystallization from acetonitrile to give **1** in 1.81 g (27%). **1**: dark yellow needles. Mp 194.2–194.5 °C. ^{1}H NMR (CD_2Cl_2): for *imino–enamine form*; δ 2.32 (s, 6H), 5.66 (s, 1H), 7.01 (bd, *J*=7.9 Hz, 4H), 7.17 (d, *J*=7.9 Hz, 4H), 7.38–7.46 (m, 2H), 7.54–7.64 (m, 2H); for *imino–imino* form; δ 2,32 (s, 6H), 3.15 (s, 2H), 6.73 (d, *J*=8.3 Hz, 2H), 7.12 (d, *J*=8.3 Hz, 2H),, 7.67 (m, 2H), 8.51(m, 2H). ^{13}C NMR (CD_2Cl_2), coexistence of imino–enamine and imino–imino tautomers, δ 20.93, 20.95, 33.61, 89.60, 119.75, 121.53, 122.86, 129.32, 130.03, 132.89, 133.94, 134.11, 144.28, 149.32, 166.92. MS (*m*/*z*) 324 (M^+), 323, 218. Anal. Calcd for $C_{23}H_{20}N_2$; C, 85.19; H, 6.17; N, 8.64. Found: C, 85.34; H. 6.21; N, 8.57.

Hydrocholide of **1** was obtained by recrystallization of **1** from an acetonitrile solution, to which a few drops of hydrochloric acid were added.

Compound (**1H**$^+$)(**Cl**$^-$): dark red prisms. Mp 245–247 °C. ^{1}H NMR (CD_2Cl_2): δ 3.42 (s, 1H), 7.02 (m, 2H), 7.24 (d, *J*=8.2 Hz, 4H), 7.47 (d, *J*=8.2 Hz, 4H), 8.32 (br s, 2H). MS (*m*/*z*) 324 (M^+), 323, 218, Anal. Calcd for $C_{23}H_{21}N_2Cl$: C, 76.56; H, 5.83; N, 7.77. Found: C, 76.28; H, 6.01; N, 7.92.

*4.1.2. 1-(p-Tolylimino)-2-(1-pyridyl)-3-(p-tolylamino)-1H-inden (**2**).* To a solution of 2-pyridyl-1,3-indandione 2.0 g, 8.9 mmol in chlorobenzene (200 mL) were added *p*-toluidine (1.92 g, 17.9 mmol) and titanium tetrachloride (2 mL) at room temperature. The mixture was heated at reflux for 4 h. Aqueous work up, extraction with dichloromethane, and drying over Mg_2SO_4 afforded a reddish solution. After the solvent was removed under reduced pressure, the product mixture was chromatographed using silica gel with benzene and dichloromethane as eluents to give 1.26 g (35%) of **2**.

Compound **2**: orange needles. Mp 235.6 °C. ^{1}H NMR (CD_2Cl_2): δ 2.41 (s, 6H), 6.47 (br s, 1H), 6.66 (br s, 1H), 6.88 (br s, 4H), 6.95 (br s, 2H), 7.00 (t, *J*=5 Hz, 1H), 7.20 (br s, 4H), 7.67 (t, *J*=5 Hz, 1H), 8.47 (d, *J*=5 Hz, 1H), 8.90 (d, *J*=7 Hz, 1H), 12.62 (br s, 1H). MS (*m*/*z*) 401 (M^+), 295, 201. ^{13}C NMR ($CDCl_3$): δ 20.99, 21.02, 96.12, 106.12, 118.71, 118.93, 122.54, 122.79, 125.11, 125.61, 128.32, 128.90, 129.58, 132.17, 132.60, 135.42, 136.12, 137.35, 138.19, 146.47, 150.01, 156.14, 156.45, 162.23. Anal. Calcd for $C_{28}H_{23}N_3$: C, 83.79; H, 5.74; N, 10.47. Found: C, 83.58; H, 5.88; N, 10.51.

*4.1.3. 1-(p-Butylphenylimino)-2-(1-quinolyl)-3-(p-butylphenylamino)-1H-inden (**3**).* Compound **3** was prepared in 41% yield from

quinolinyl-1,3-indandione (quinoline yellow) and *p*-butylaniline in a similar manner to that described for **2**:**3**: orange solid. Mp 192–195 °C. ^{1}H NMR ($CDCl_3$): δ 0.96 (t, J=7.3 Hz, 1H), 1.41 (sextet, J=7.3 Hz, 2H), 1.66 (p, J=7.3 Hz, 2H), 2.67 (dt, J=7.3 Hz, 2H), 6.49 (d, J=7.0 Hz, 1H), 6.76 (d, J=7.3 Hz, 1H), 6.91 (t, J=6.8 Hz, 1H), 6.94 (d, J=7.6 Hz, 2H), 6.96 (t, J=7.6 Hz, 1H), 7.18 (d, J=7.6 Hz, 2H), 7.23 (d, J=7.6 Hz, 2H), 7.30 (d, J=7.6 Hz, 1H), 7.40 (t, J=7.4 Hz, 1H), 7.58 (t, J=7.4 Hz, 1H), 7.71 (d, J=7.9 Hz, 1H), 7.86 (d, J=7.9 Hz, 1H), 7.04 (d, J=9.0 Hz, 1H), 9.16 (d, J=9.0 Hz, 1H), 13.85 (br s, 1H). ^{13}C NMR ($CDCl_3$): δ 14.06, 14.12, 22.25, 22.36, 33.73, 33.96, 35.09, 35.17, 105.29, 118.79, 121.59, 122.97, 124.58, 125.27, 125.51, 126.84, 127.39, 128.75, 128.98, 129.01, 129.05, 132.74, 135.42, 137.19, 137.39, 137.57, 140.68, 145.82, 149.99, 156.44, 157.75, 162.16. MS (m/z) 535 (M^+), 306,288. Anal. Calcd for $C_{38}H_{37}N_3$. C, 85.20, H; 6.96, N, 7.84. Found: C, 85.23, H, 6.98, N, 7.58.

The X-ray crystallographic data were collected at cryogenic temperature (−50 °C for **1**, −100 °C for (**1H**$^+$)(**Cl**$^-$), −180 °C for **2**) on a Rigaku AFC 5S diffractometer, using graphite monochromatised Mo–Kα radiation (λ=0.71073 Å). Crystal data have been submitted to CCDC. Crystal data for **1**: $C_{23}H_{20}N_2$, $P2_1/c$, a=6.5904(19), b=18.541(7), c=14.561(4), β=90.304(11), V=1779.2(9) Å^3, Z=4, D_{calcd}=1.211 g/cm^3, R_1=0.0413, wR_2=0.0460, CCDC-7,49,201. Crystal data for (**1H**$^+$)(**Cl**$^-$): $C_{23}H_{21}N_2Cl$, P-1, a=8.576(5), b=10.508(6), c=11.728(6), α=107.06(2), β=102.246(19), γ=107.83(2), V=907.5(8) Å^3, Z=2, D_{calcd}=1.321 g/cm^3, R_1=0.0461, wR_2=0.0830, CCDC-749202. Crystal data for **2**: $C_{28}H_{23}N_3$, Pnma, a=20.7671(14), b=19.3314(3), c=5.10301(10), V=2048.63(15) Å^3, Z=4, D_{calcd}=1.302 g/cm^3, R_1=0.0432, wR_2=0.0582, CCDC-749203.

Theoretical calculations have been performed by using Gaussian 03 program package.[16] The density functional theory (DFT) was employed for the full geometric optimizations at the B3LYP/6–31G(d,p) level.

Acknowledgements

This work was partially supported by a Grant-in-Aid for Scientific Research (C) from MEXT (No. 21550048).

References and notes

1. Claramunt, R. M.; Elguero, J.; Katritzky, A. R. In *Advances in Heterocyclic Chemistry*; Katritzky, A. R., Ed.; Academic: San Diego, 2000; Vol. 77, pp 1–50.
2. (a) Kendrick, R. D.; Friedrich, S.; Wehrle, B.; Limbach, H. H.; Yannoni, C. S. *J. Magn. Reson.* **1985**, *65*, 159; (b) Limbach, H. H.; Wehrle, B.; Zimmermann, H.; Kendrick, R. D.; Yannoni, C. S. *J. Am. Chem. Soc.* **1987**, *109*, 929; (c) Limbach, H. H.; Hennig, J.; Kendrick, R.; Yannoni, C. S. *J. Am. Chem. Soc.* **1984**, *106*, 4061.
3. Thoburn, J. D.; Luttke, W.; Benedict, C.; Limbach, H.-H. *J. Am. Chem. Soc.* **1996**, *118*, 12459.
4. Sugawara, T.; Takasu, I. In *Advances in Physical Organic Chemistry*; Bethell, D., Ed.; Academic: San Diego, 1999; Vol. 38, pp 219–273.
5. (a) Larina, L. I.; Sorokin, M. S.; Albanov, A. I.; Elokhina, V. N.; Protsuk, N. I. *Magn. Reson. Chem.* **1998**, *36*, 110; (b) Elguero, J.; Cano, F. H.; Foces-Foces, C.; Llamas-Saiz, A. L.; Limbach, H.–H.; Aguilar-Parrilla, F.; Claramunt, R. M.; Lopez, C. *J. Heterocycl. Chem.* **1994**, *31*, 695; (c) Foces-Foces, C.; Hager, O.; Jagerovic, N.; Jimeno, M. L.; Elguero, J. *Chem. Eur. J.* **1997**, *3*, 121; (d) Lunazzi, L.; Parisi, F.; Macciantelli, D. *J. Chem. Soc., Perkin Trans. 2* **1984**, 1025.
6. Elguero, J.; Katritzky, A. R.; Denisko, O. V. In *Advances in Heterocyclic Chemistry*; Katritzky, A. R., Ed.; Academic: San Diego, 2000; Vol. 76, pp 1–84.
7. Stanovnik, B.; Tisler, M.; Katrizky, A. R.; Denisko, O. V. In *Advances in Heterocyclic Chemistry*; Katritzky, A. R., Ed.; Academic: San Diego, 2006; Vol. 91, pp 1–134.
8. (a) Raczynska, E. D.; Gawineoki, R. *Trends Org. Chem.* **1998**, *7*, 85; (b) Anulewicz, R.; Wawer, I.; Krygowski, T. M.; Mannle, F.; Limbach, H.-H. *J. Am. Chem. Soc.* **1997**, *119*, 12223; (c) Ito, K.; Kizuka, Y.; Hirano, Y. *J. Heterocycl. Chem.* **2005**, *42*, 588.
9. (a) Lycka, A.; Frebort, S.; Almonasy, N. *Tetrahedron Lett.* **2008**, *49*, 4213; (b) Seckarova, P.; Marek, R.; Malinakova, K.; Kolehmainen, E.; Hockova, D.; Hocek, M.; Sklenari, V. *Tetrahedron Lett.* **2004**, *45*, 6259; (c) Siri, O.; Braunstein, P.; Rohmeer, M.-M.; Benard, M.; Weiter, R. *J. Am. Chem. Soc.* **2003**, *125*, 13793; See also Claramunt, R. M.; Lopez, C.; Maria, M. D. S.; Sanz, D.; Elguero, S. J. *Prog. Nucl. Magn. Spectrosc.* **2006**, *49*, 169.
10. Ferguson, G.; Parvez, M.; Lloyd, D.; Marshall, D.; Potter, D. *Acta Crystallogr.* **1986**, *C42*, 912.
11. Coalescence method is applicable to two singlets representing interchange between two equivalent sites. Therefore, the value estimated herein is an approximate one.
12. Yavari, I.; Adib, M.; Jahani-Moghaddam, F.; Bijamzadeh, H. R. *Tetrahedron* **2002**, *58*, 6901.
13. Dobosz, R.; Kolehmainen, E.; Valkonen, A.; Osmialowski, B.; Gawinecki, R. *Tetrahedron* **2007**, *63*, 9197.
14. In ^{1}H NMR, the methylene protons at the α position of the butyl substituent appear as a quartet, which is attributed to overlap of two triplets. This means that the methylene protons adjacent to the benzene ring suffer the most significant magnetic nonequivalence among three sets of methylene protons in the butyl group, in contrast to the ^{13}C NMR signals.
15. Yavari, I.; Adib, M.; Bijanzadeh, H. R.; Sadegi, M. M. M.; L-Khouzani, H.; Safari, J. *Monatsh. Chem.* **2002**, *133*, 1109.
16. Frisch, M. J.; Trucks, G. W.; Schlegel, H. B.; Scuseria, G. E.; Robb, M. A.; Cheeseman, J. R.; Montgomery, J. A., Jr.; Vreven, T.; Kudin, K. N.; Burant, J. C.; Millam, J. M.; Iyengar, S. S.; Tomasi, J.; Barone, V.; Mennucci, B.; Cossi, M.; Scalmani, G.; Rega, N.; Petersson, G. A.; Nakatsuji, H.; Hada, H.; Ehara, M.; Toyota, K.; Fukuda, R.; Hasegawa, J.; Ishida, M.; Nakajima, T.; Honda, Y.; Kitao, O.; Nakai, H.; Klene, M.; Li, X.; Knox, J. E.; Hratchian, H. P.; Cross, J. B.; Bakken, V.; Adamo, C.; Jaramillo, J.; Gomperts, R.; Stratmann, R. E.; Yazyev, O.; Austin, A. J.; Cammi, R.; Pomelli, C.; Ochterski, J. W.; Ayala, P. Y.; Morokuma, K.; Voth, G. A.; Salvador, P.; Dannenberg, J. J.; Zakrzewski, V. G.; Dapprich, S.; Daniels, A. D.; Strain, M. C.; Farkas, O.; Malick, D. K.; Rabuck, A. D.; Raghavachari, K.; Foresman, J. B.; Ortiz, J. V.; Cui, Q.; Baboul, A. G.; Clifford, S.; Cioslowski, J.; Stefanov, B. B.; Liu, G.; Liashenko, A.; Piskorz, P.; Komaromi, I.; Martin, R. L.; Fox, D. J.; Keith, T.; Al-Laham, M. A.; Peng, C. Y.; Nanayakkara, A.; Challacombe, M.; Gill, P. M. W.; Johnson, B.; Chen, W.; Wong, M. W.; Gonzalez, C.; Pople, J. A. *Gaussian 03 Rev.C02*; Gaussian,: Wallingford CT, 2004.